BJES Basrah Journal for Engineering Sciences

Basrah Journal for Engineering Sciences, Vol. 23, No. 1, (2023), 106-116

Original Article

Journal homepage: www.bjes.edu.iq
ISSN (Online): 23118385, ISSN (Print): 18146120

OPEN ACCESS

Experimental and Numerical Study the Linear Stress Analyses for the Prediction of Fracture Toughness of Ductile Material

Sara A. Khudair [1,2]*, Atheed H. Taha [3], Ameen A. Nassar [4]

[1,3] *Department of Mechanical Engineering, College of Engineering, University of Basrah, Basrah, Iraq*
[2] *Department of Material Engineering, College of Engineering, University of Basrah, Basrah, Iraq*
E-mail addresses: sarakhdhierl@gmail.com , atheed.taha@uobasrah.edu.iq , ameen.nassar@uobasrah.edu.iq
Received: 11 August 2022; Revised: 17 September 2022; Accepted: 26 September 2022; Published: 2 July 2023

Abstract

The purpose of this paper is to determine a stress intensity factor experimental and numerically in the linear region by using a CT specimen of ductile material with a thickness of 15 mm, a width of 30 mm, and pre-crack 1.3 mm this dimension according to ASTM-E399-12 [1], by pulling the specimen in a 600 kN universal testing machine at a very slow speed rate of 0.5 mm/min. The load is applied until the fracture is accrued, the computer-controlled universal testing machine gives the value of the load and the displacement transducer gives a crack mouth opening displacement. The result showed experimental K_I is equal to 75.412 MPa$\sqrt{m}$, and numerical K_I is equal to74.576 MPa$\sqrt{m}$, this test showed a very slight decrease in FEA stress intensity factor compared to that in an experimental result which means the stress intensity factor, K_I remains very close between experimental and numerical with an error percentage of about (1.12 %). The finite element analysis provides the best approximation to true fracture toughness values, and it can be used to acquire close parameters if experimental testing is not possible.

Keywords: SIF, ANSYS, FEM, Low carbon steel.

https://doi.org/10.33971/bjes.23.1.14

1. Introduction

The ability to predict the fracture toughness of most metallic materials is a critical factor to consider when constructing engineering structural components such as pipes, flow tanks, and pressure vessels. AISI 1010 carbon steel (mild steel) is widely used in a wide range of engineering applications it is tough, malleable, ductile, and more elastic than wrought iron. the study of the mechanical characteristics and fracture behavior of this type of metal is important and useful to designers who utilize it in their work. The fracture toughness is predicted using ASTM-E399-12 [1], which is used to predict linear fracture toughness (stress intensity factor K_I) for ductile materials that undergo large plastic deformation.

In fracture mechanics that characterize a material's ability to resist crack propagation in the presence of a crack, and it is one of the most essential aspects of any material in many engineering design applications.

Fracture is an issue that humanity has dealt with for as long as man-made structures have existed, and it is a branch of solid mechanics that explains how bodies with cracks behave under various loading circumstances. Cracks in a material may happen during processing, manufacture, or service, or as a result of the nature of the loads acting on the structure. If a crack exists in a structural member, the component becomes weak, and later fracture occurs. The presence of these defects in the components causes problems that can adversely affect the safety of the structural components and reduce their service life.

As a result, the Fracture Mechanics approach was created to determine if these little defects could expand into larger cracks, resulting in catastrophic failure of these structural components. Fracture Mechanics analysis becomes quite important for all engineers who are studying the reasons for structural component failure in numerous scientific fields.

The stress distribution at cracks, particularly at the crack tip, can be used to make accurate predictions about the repercussions of a crack that could lead to rapid fracturing [2], [3].

The fracture occurs when the stress intensity factor is equal or greater than plane strain fracture toughness according to Elastic Plastic Fracture Mechanic theory, or the fracture occurs when the stress intensity factor is equal or greater than plane stress fracture toughness, according to Linear Elastic Fracture Mechanic theory, i.e. crack propagation occurs when $K_I > K_{IC}$ or $K_I > K_C$. As a result, engineers can design a structure with stress intensity factors corresponding to distinct fracture modes utilizing (LEFM) theory, which is limited by (plain strain conditions and Small-Scale Yielding) as illustrated in Fig. 1. Engineers can create a structure that has stress intensity factors that correspond to various fracture modes. While the stress intensity factor does not accurately describe the true fracture mode beyond the elastic zone, the Non-Linear Elastic-Plastic Fracture Mechanics theory must be applied after this region, as shown in Fig. 1, where u is the crack length and F is the applied force.

The CTOD-Model and the J-Integral Model are two main branches of Elastic-Plastic Fracture Mechanics [4].

The fracture toughness was the subject of several studies. Some of these an experimental and others numerical works.

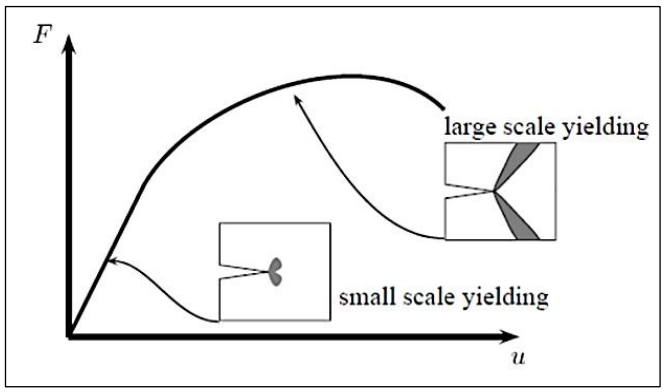

Fig. 1 plastic zones of cracked structures [4].

Kulkarn et al. 2002 [5] introduced a three-dimensional experimental finite element model to a recently built model to predict the fracture toughness in thin metal sheets (CTOD Model). They used the dugdual model to estimate the elastic component of CTOD under conditions of plane strain, and they used the plastic hinge model to estimate the plastic component. They concluded that there is good agreement between FE results and experimental data (within 1-4 %).

Ping et al. 2006 [6] used the ANSYS software to analyze the beryllium compact tension specimen that was designed following ASTM E-399-12 fracture characteristics near the crack tip. Due to the symmetry of the beryllium compact tension specimen, using a half model and element type (Plane-82). They concluded that the experimental value and the FEA-calculated fracture toughness value, which is 19.1 MPa/m, are basically identical to the experimental value.

Nagoju and Gopinath 2013 [7] used the SIF K_I in the 2D structure of ASTM A36 steel was determined using the displacement extrapolation technique, and the results were compared to theoretically derived SIF. The important factor is the critical crack length, which is predicted to be 40 mm, 34 mm, and 28 mm for loads of 250 N/mm^2, 275 N/mm^2, and 300 N/mm^2, respectively. This study showed that when crack length increased, the SIF value increased as well. When the SIF reached its critical value or fracture toughness, the component failed.

Beltran et al. 2014 [8] computed the critical stress intensity factor for structural steel pipes API-5, according to conditions of (LEFM). According to the ASTM E-399 standard, the material was evaluated for fracture toughness using fatigue crack propagation on a standardized compact specimen (CT). A crack size (a) of 0.5 w and a thickness (B) of (W/4) were selected. The specimens were subjected to fatigue pre-cracking by application of repeated cycles of load in tensile-tensile and constant load amplitude with a load ratio of R = 0.1. The experimental Compliance method was used based on data obtained from load vs. Crack Mouth Opening Displacement (CMOD). The results show a stress intensity factor of 35.88 MPa$\sqrt{\text{m}}$ for a 25 mm crack size specimen. ANSYS workbench 14.5 fracture module was used to perform a finite element analysis on compact specimens to determine the parameter. The study produced showed values for closeness to the experimental findings. The finite element analysis provides the best approximation to true fracture toughness values, according to experimental and simulated data, and it can be used to acquire close parameters if experimental testing is not possible.

Soltysiak et al. 2016 [9] compare the crack length (a) as a function of the crack opening displacement (δ) which was determined by experimental and numerical methods. Using a titanium alloy (CT) specimen constructed of Ti6Al4V, tests were done at room temperature in a laboratory. The fatigue crack's length was measured using both the updated Fatigue VIEW system and the original program designed for crack length analysis. ABAQUS software was used to run numerical testing. If using the Fatigue VIEW system to measure the fracture length proves difficult, further study will focus on developing a hybrid tool. When curves of (a) and (δ) computed numerically and experimentally are as closely related to one another as possible, the tool provided can perform to its maximum potential. The achieved crack length estimation error for the numerical techniques in the experiments provided up to the crack length of a = 20 mm was 13,0 percent for the force PMAX 11 = 6,31 kN and 7,3 percent for the force PMAX 02 = 10,76 kN, respectively.

Abdulsada 2018 [10] introduced studying experimentally some mechanical properties, stress intensity factor, and the crack mouth opening displacement CMOD for the base and welded low carbon steel metal using single edge crack tension SECT, using the capabilities of Finite Element ABAQUS software and the Extended Finite Element Method (XFEM) capabilities to determine the numerical results of the tensile test and the test single edge crack tension SECT 3D analysis of specimens. The validation of the numerical analysis was performed by the experimental study. Finally, the numerical results are compared with the results of the experiment, and the simulation results demonstrated a good agreement with the experimental results.

Recently, Nassar and Fayyad 2019 [4] used the ASTM-E-399 specification for compact tension specimens for real-world design issues, the fracture toughness in the elastic stage is directly predicted by the ANSYS software. However, in the elastic-plastic region, the crack tip opening displacement model (CTOD-Model) is used to estimate the fracture toughness using a three-point bend specimen following ASTM-E-1290. After extracting load-displacement data from the ANSYS software and using it in the (CTOD-Model), which is divided into two components, elastic and plastic, the critical value for crack tip opening displacement will be calculated. The elastic component has been estimated using the Dugdual Model, while the plastic component will be estimated using the Plastic Hinge Model. Nevertheless, the fracture toughness value predicted by using the finite element approach from non-linear elastic and non-linear elastic-plastic studies provides good results that are highly close to the experimental values with an error ratio between (10 % to 14 %).

Wester and Gunnarsson 2020 [11] showed the possibilities of a modeling and recreating the fracture toughness test E399 using available test data. It also adds to the conclusion that for an excessive amount of plasticity the 95 % secant cannot be used to derive K_{IC} as the crack has not propagated at that point. Further, it has been shown that for a limited amount of plasticity the J-integral can be used to calculate the linear elastic stress intensity factor. The thesis also discusses the validity of adding friction between the specimen and the pin to increase the stiffness in the simulation. Finally, ways of using FE modeling.

Khdir 2020 [12] explained how to use the finite element method to calculate the stress intensity factors for steel plates of various thicknesses with an elliptical hole in the middle and various stresses applied to them. The stresses at the crack tip have an influence on the failure of the cracked parts. The stress intensity factor K can be used to calculate the stress

contribution. Numerous solid-type elements and nodes are numerically modeled using the ANSYS software in this work. For a more accurate result, a finer mesh is employed in the vicinity of the crack tip. The output from ANSYS can then be used to calculate an error percentage. The study produced showed the stress has been changed by the plate's thickness increasing the plate thickness resulting in increasing the SIF at the location of the crack tip. Also, the thickness of the plate has a significant effect on the stress distribution over the whole plate.

2. Fracture toughness concept

It has been found that materials fail at a critical magnitude of K_I, called the critical stress intensity or fracture toughness, K_{IC} [11]. The fracture toughness of a material is dependent on temperature, corrosive environment, boundary effects, etc. The fracture criterion can be stated as fracture toughness is a measure of a material's resistance to physical separation generated by a process of unstable macro-crack propagation in physical science. It is a material mechanical parameter that should not change with changes in specimen size, loading speed, temperature, or other factors. Fracture toughness is an experimental material component measured by one or more of various standard fracture toughness test techniques in material science, and it is one of the most important parameters for evaluating the mechanical properties of any material for practically all design applications [4].

2.1. Fracture toughness parameters

There are three common fracture toughness measurements for linear and non-linear fracture mechanics. These measurements are established in dealing with fracture of cracked solids: linear elastic fracture mechanics (LEFM), which uses the stress intensity factor K_I, elastic-plastic fracture mechanics (EPFM), which uses the J-Integral, and the crack tip opening displacement (CTOD) method. These measurements of fracture toughness.

When a material behaves in a linear elastic manner, prior to failure, such that the plastic zone is small compared to the specimen dimension, the stress intensity factor (K_I) describes the stress at the crack tip in mode I loading. It was proposed by Irwin in 1957 [13].

2.2. Stress intensity factor (K_I)

The stress-intensity factor K_I is a parameter that quantifies the state of stress near the crack tip in a linear elastic material [11]. Because residual stresses were loaded remotely, it was especially important to calculate the stress intensity factor near the crack tip. The (SIF) is a theoretical number frequently used to describe a homogeneous linear elastic fracture mechanics (LEFM) material, and it is useful for defining criteria for failure for delicate materials [14]. It is necessary to understand the critical crack size and a characteristic that describes a crack's ability to expand such a variable need to be able to relate the results of laboratory tests or analyses to the functioning of structures. As a result, analysis or laboratory test results can be used to forecast how a structure with cracks will react. The fracture size, structural geometry, and loading conditions all play a role in determining this parameter, also known as the stress intensity factor (K_I). Different forms and numbers of cracks are frequently found in structural components under a variety of loads and boundary circumstances in actual engineering situations. Therefore, the presence of a fracture could have a significant impact on a structure's strength, because flaws are inevitable in a process that produces products at a reasonable cost. In the majority of constructions, cracks may be discovered or created during service in areas of concentrated stress, and the fracture may be large enough for the crack tip to be closer to a boundary. Due to the low stress acting on the structure, the crack may propagate and lead to structural failure. The most fundamental variable in fracture mechanics is the stress intensity factor (SIF), which determines whether a crack will propagate within a cracked structure under specific loading conditions. It also determines the crack's stability. SIF can be calculated very easily for relatively basic components and loadings, but problems may occur when dealing with complex fractured structures [15].

On the other hand, the critical value of this parameter known as fracture toughness which is a property of the material is determined from laboratory tests. By equating this parameter to its critical value relation between applied load, crack size, and structure geometry can be obtained. Fracture toughness can be defined as the ability of the material to resist fracture in the presence of cracks. It is similar to the yield strength of the material which measures the resistance of the material to yield stress intensity factor K for the linear elastic region for low carbon steel AISI1010 calculation used Eq. (1) [10].

$$K_I = \sqrt{CMOD\,\sigma_y\,E} \tag{1}$$

Or in another form according to ASTM-E399 the stress intensity factor at the (Q) point (K_Q) is calculated as Eq. (2)[1].

$$K_Q = \frac{P_Q\, f(a/w)}{\sqrt{B\,B_N\,w}} \tag{2}$$

The two principles of fracture mechanics are linear elastic fracture mechanics (LEFM), which takes into account the foundations of linear elasticity theory, and plastic fracture mechanics (PFM), which is used to describe the plastic behavior of ductile objects. The Linear Elastic Fracture Mechanics (LEFM) theory can only account for plastic deformation upstream of the crack tip. A large plastic zone size ($r_P << a$), otherwise a large plastic zone size ($r_P \geq a$) governs the fracture process according to the Elastic-Plastic Fracture Mechanics (EPFM) theory [16].

3. Experimental protocol

3.1. Aim of the experiments

1. Determine the stress intensity factor experimental and numerically by the ANSYS software.
2. Determined the crack mouth opening displacement (CMOD) by using displacement transducers (data logger device) connecting with a computer to the INSTRON tensile machine.
3. Study experimentally some mechanical properties.
4. Determine the error between experimental and numerical stress intensity factors.

3.2. Materials selection

AISI 1010 Low carbon steel that is used in this investigation with a thickness of 15 mm (0.590 in) is used as a base metal for the experimental work. The plate of carbon steel (AISI1010) with dimensions of (450 × 50) mm was purchased from the industrial scrap market. The plate was machined and cleaned to remove dirt and oxides in the workshop of the College of Engineering, University of Basrah to get on the required sample for the required experimental tests.

Applications: Rods, valves, gears, crankshafts, connecting rods, railway axles, and other components are made of it.

3.3. The chemical composition tests

This test aims to estimate the required chemical properties of the selected material. One small specimen plate of carbon steel shown in Fig. 2 (a) was analyzed to examine it is chemical composition by using the Spectrometer device as shown in Fig. 2 (b).

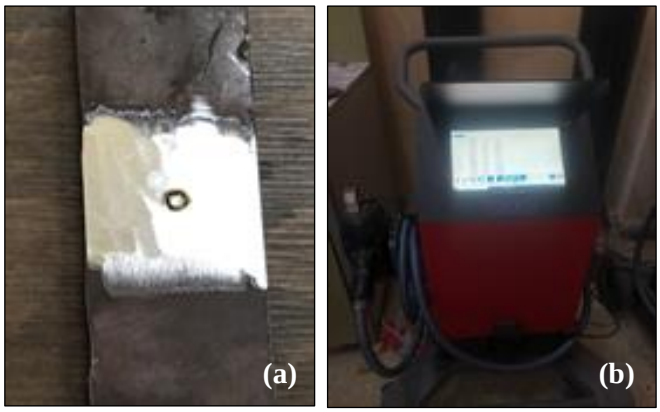

Fig. 2 (a) small piece of metal, **(b)** Spectrometer device.

3.4. Mechanical properties

3.4.1. Tensile test

One of the most significant and commonly analyzed characteristics of materials is the ability to stand cracking under tensile stress. To determine the tensile strength, a computerized universal testing machine is used, and three tensile specimens are prepared using a lathe machine following the ASTM (E8/E8M-9) [17] standard with all dimensions in mm shown in Fig. 3. The machine device of 600 kN capacities used in this test was Instron Tensile Machine with fully controlled computer programming as shown in Fig. 4. The specimen is placed in the tensile machine until the specimen is fractured as shown in Fig. 5.

In a tensile test, a specimen is fixed to the end of the grippers which is connected to the upper plate and lower plate of the tensile machine.

To determine the material's ultimate tensile strength, a specimen is extended up to it is breaking point using a controlled system connected to the Instron Tensile Machine.

During the experiment, the amount of force applied (F) and the sample elongation (L) is measured. Material characteristics are commonly described using the terms stress (force per unit area) and strain (change in length to the original length). The results stress vs strain graph is plotted as shown in Fig. 6. The program placed on the *PC* connected to the tensile machine recorded all load and displacement data during the test.

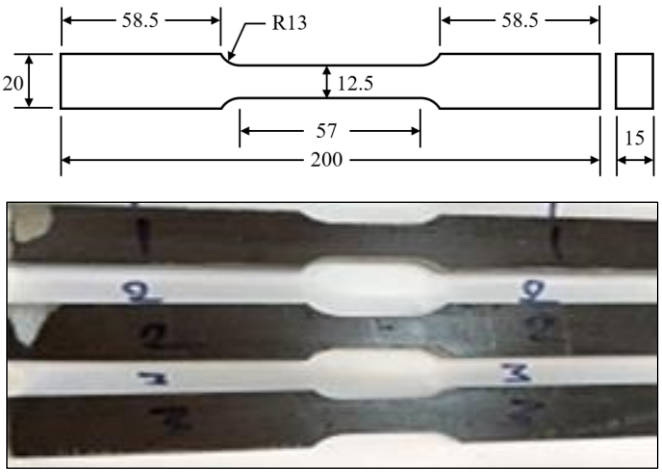

Fig. 3 Dimension tensile test specimens before fracture.

Fig. 4 Instron tensile test machine.

Fig. 5 Tensile test specimens after a fracture.

To assess the tensile properties of low carbon steel, tensile tests were carried out as per ASTM (E8/E8M-9) standards, and a total of three test specimens have been prepared. Table .1 shows the best result obtained.

Table 1. the mechanical properties of low carbon steel.

Thickness (mm)	**Yield stress (MPa)**	**Ultimate tensile stress (MPa)**	**Modulus Elasticity *E* (GPa)**	***v***
15	287.8	433.6	200	0.3

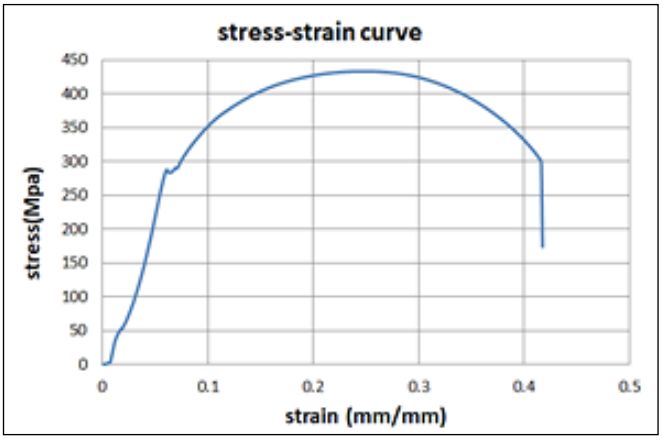

Fig. 6 Stress-strain curve.

The chemical composition of the material as presented in the test is shown in Table 2.

Table 2. the chemical composition of low carbon steel.

Element	C	Si	MN	P	S	Cr	Fe
Percentage	0.097	0.234	0.69	0.003	0.002	0.011	98.8

3.4.2. Fracture toughness specimen (CT) preparation

There were three stages to the preparation using the WEDM machine this machine is controlled by AutoCAD software. Water and oil were used as the dielectric using a 0.18 mm diameter molybdenum wire, and a specimen was machined to have the specified dimensions and configuration of the compact tension. In the first stage, a 0.18 mm diameter wire was used to the specimen's profile according to the dimensions. Following that, a 0.18 mm diameter wire was used to introduce the 1.3 mm pre-crack instead of fatigue pre-crack. After that, the specimens were separated from the main bar as shown in Fig. 7.

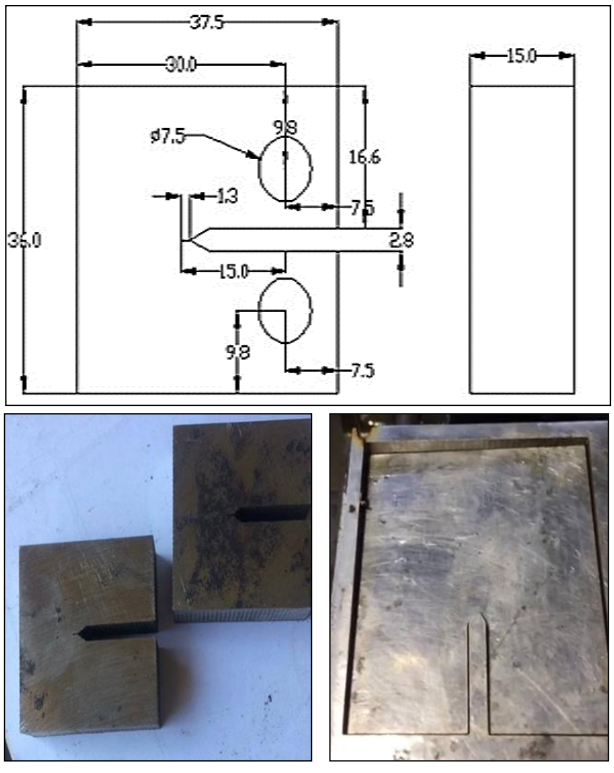

Fig. 7 Steps of preparation of *CT* specimens.

3.4.3. Pre-cracking fatigue

The main aim of fatigue pre-crack is to obtain a sharp crack. It is important in the test specimen to simulate a straight propagation of crack [13]. The theory of fracture mechanics applies to cracks that are infinitely sharp before being loaded, while laboratory specimens will always fall short of this ideal, it is important to initiate cracks that are acute enough to be useful, cyclic loading is the most efficient approach to creating such a crack. The fatigue crack must be introduced in such a way that it has no serious effect on the toughness value being tested. Because cyclic loading produces a finite-radius crack with a small plastic zone at the tip, but because this technique is costly and time-consuming, we use the WEDM to introduce this crack in the current work [18].

Fig. 8 Pre-cracking by WEDM.

3.4.4. Side grooving

On each side of the specimen, the side grooving was machined to maintain a notch angle of 60° and a depth of nearly 1.5 mm into the sidewalls of specimens seen in Fig. 9. The primary goal of the side grooving is to ensure the crack front is straight during a test. Because the material towards the outside surfaces is in a state of low-stress triaxiality a specimen without side grooves is subject to crack tunneling and shear lip formation. Side grooves remove the low triaxiality zone, resulting in relatively straight crack fronts if done correctly [17].

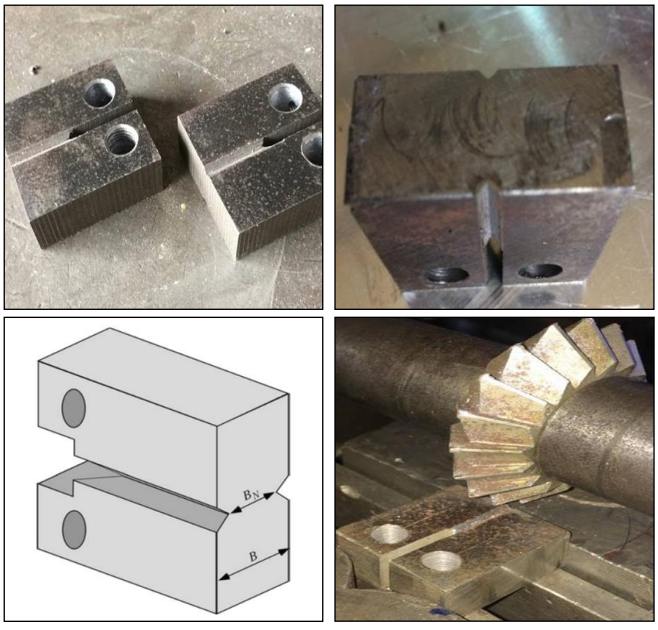

Fig. 9 side grooving.

3.4.5. Fixtures and knife blocks

The UB-5A clip is a type of displacement transducers (clip gauge) that conforms to ASTM specifications shown in Fig. 10. Figures 11 and 12 are from the protocol for designing the knife blocks to contact the clip gauge for the measured CMOD. The knifes block structure for staffing the offset clip gauge is designed to conform to ASTM-E 399 standards for measuring the CMOD (displacement transducer) is shown in Fig. 13. Figure 11 shows the rotation shape in the clip gauge during the run operation test rather than linear because the angle value for the knife block edge is 60º for contact with the clip gauge edge. The knife blocks may be separate pieces affixed to the specimen as shown in Fig. 13 [10].

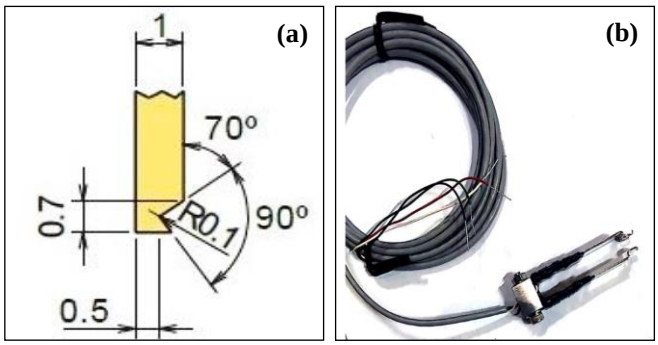

Fig. 10 (a) Received CMOD notch details [10], **(b)** the UB-5A Clip type.

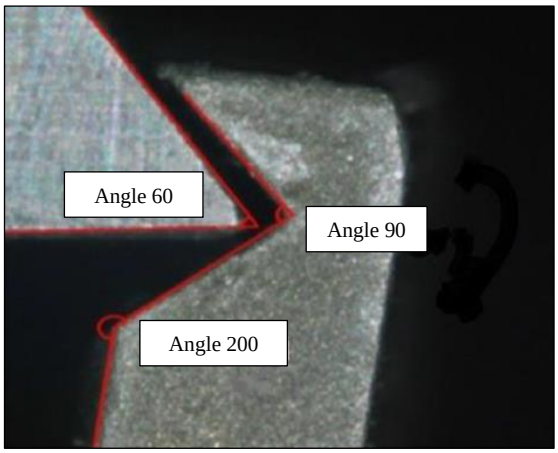

Fig. 11 As specified 60° knife edge. The near planer contact resulted in the relative motion of the contact point with the rotation of the knife edge [19].

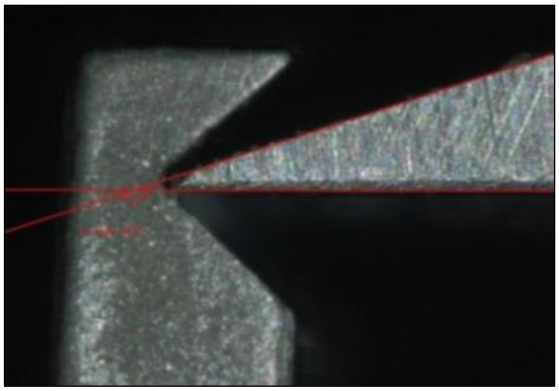

Fig. 12 Sharpened knife edge design decreased the relative motion of the contact point during the rotation. Note that the termination of the knife edges was left at 60° [19].

Fig. 13 Attachable knife-edge design.

This design features a knife-edge spacing of 5 mm (0.2 in.). The effective gauge length is established by the points of contact between the screw and the hole threads. After that, the complete specimens are shown in Fig. 14.

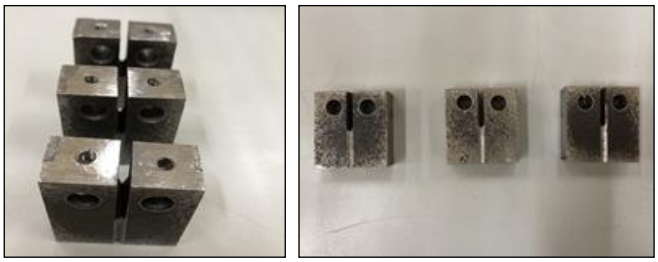

Fig. 14 Compact tension specimens.

3.4.6. Testing fixtures

A loading clevis suitable for testing standard compact tension specimen the size, proportions, and tolerances for the clevis as shown in Fig. 15 according to ASTM-E399 are all scaled to specimens with $W/B = 2$ for $B \geq 13$ mm. Both ends of the specimen are held in the clevis and loaded through pins to allow rotation of the specimen during testing. The clevis holes are provided with small flats on the loading surfaces to provide rolling contact, thereby minimizing friction effects.

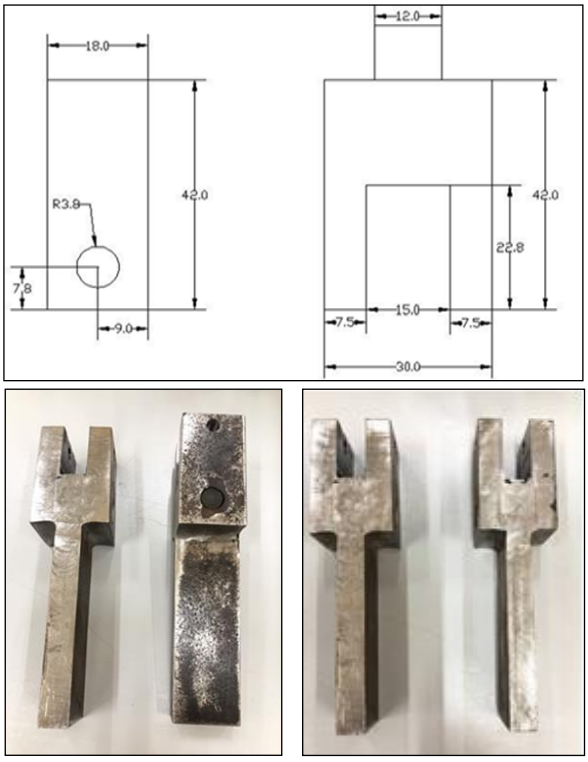

Fig. 15 Loading clevis.

4. Finite analyses

4.1. 3D FE model and boundary conditions

Finite element analysis was performed using ANSYS software 2019 R1 workbench. To compare testing results with simulation values, a compact specimen (*CT*) was simulated in a 3D model using the geometry and dimensions of the experimental specimens. The mechanical auto-generated (quad) mesh built in the workbench was used to construct the mesh, generated mesh embedded in the workbench. Figure 16 indicates the meshing in finite element analysis. The generated meshing contains 11457 elements and 51492 nodes.

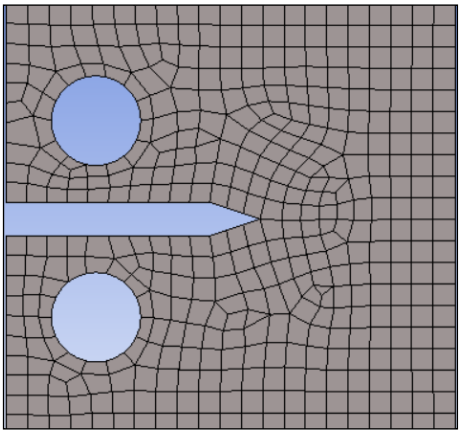

Fig. 16 Compact specimen meshing.

Because of the presence of wide stress gradients in a small zone around the crack tip. A vertex sizing meshing (sphere influence with radius 2 mm and element size 0.25 mm was realized in the proximity of the crack tip's edges to evaluate properly the stress concentration in this zone. Fig. 17 shows the vertex sizing meshing. The boundary conditions may be applied to the fixed supported in the lower hole of the pin and added to the components that loaded the specimen in the load *y*-axis by 12.606 kN in the higher hole of the pin shown in Fig. 18. Pre-meshed crack with nodes placed at the crack front line was how the crack was described.

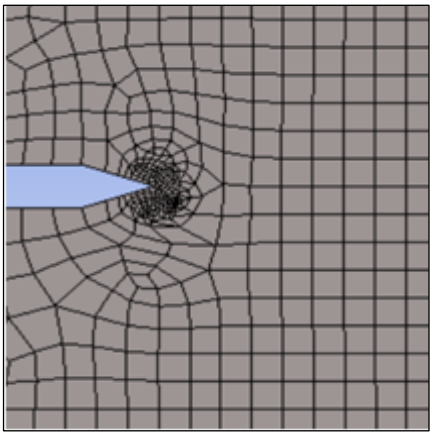

Fig. 17 Vertex size meshing at the crack tip.

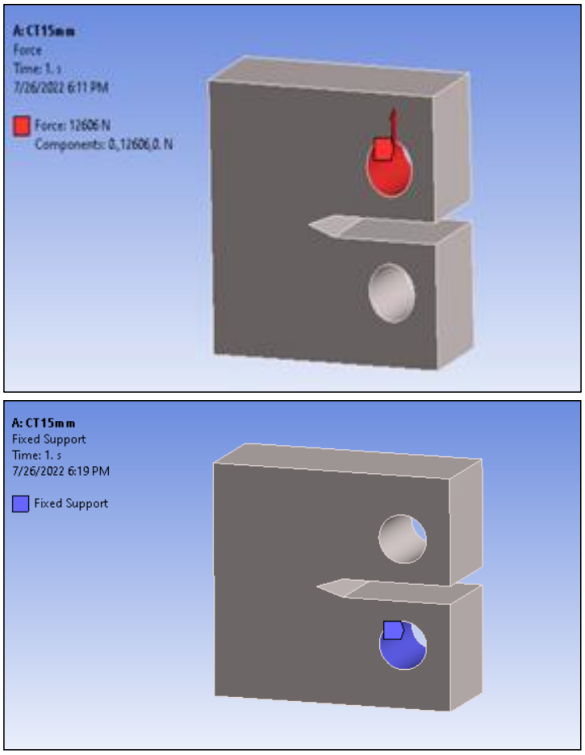

Fig. 18 B.C of the specimen.

4.2. Testing procedure

This test method covers procedures and guidelines for the determination of fracture toughness of metallic materials using the following parameters K_I. The fracture toughness determined following this test method is for the opening mode I of loading.

The present experimental work was performed on the modified compact tension (*CT*) specimen, by pulling the specimen in a 600 kN universal testing machine at a very slow speed rate of 0.5 mm/min. The load is applied until the fracture is accrued as shown in Fig. 19. The computer-controlled universal testing machine gives the value of the load, and the displacement transducer gives a crack mouth opening displacement.

Fig. 19 Specimens during the test and after a fracture.

5. Result and discussion

5.1. Load and CMOD results

The specimen was loaded under tension at the same time as the tensile operation. The data were recorded when the metal specimen was loaded into a universal tensile machine, the load was recorded from the program placed on the *PC* connected to the tensile machine but the CMOD recorded from the displacement transducer during the load's amount difference in the same time at the room temperature as shown in Fig. 20 and data as indicated in Table 3. The specimen was found to have a CMOD of 0.002 mm at a load of 0.502 kN and a CMOD of 0.417 mm at a load of 12.606 kN these data were in the linear elastic region and the other data in the plastic region.

Fig. 20 *PC* and displacement transducer.

Table 3. Load-CMOD data.

NO	P (kN)	CMOD (mm)
1	0	0
2	0.5821	0.002
3	0.953	0.018
4	4.5859	0.084
5	9.1748	0.209
6	12.606	0.417
7	13.956	0.961
8	15.084	1.564
9	16.037	2.115
10	16.823	2.752
11	17.419	3.319
12	17.784	4.066
13	17.642	4.496
14	16.483	4.501
15	14.589	4.504
16	11.554	4.506

The load vs. CMOD (Crack Mouth Opening Displacement) graphic is displayed in Fig. 21. The curve shows normal behavior, showing a linear pattern during the initial loading stage and non-linear in a second stage with significant CMOD increases but a low load increase.

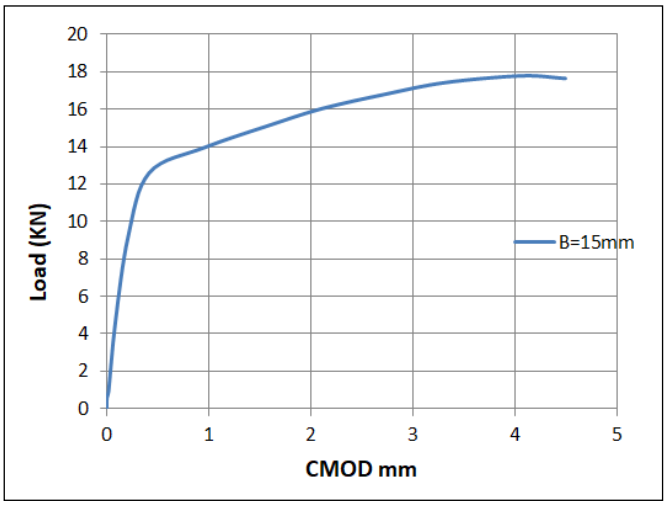

Fig. 21 load-CMOD curve for the metal.

5.2. Calculation of the stress intensity factor

The stress intensity factor K_I in the linear elastic region for low carbon steel AISI1010 according to Eq. (1) is shown in Table 4. Figure 22 shows the relationship between stress intensity factor K_I and CMOD, and the relationship between load and stress intensity factor K_I is shown in Fig. 23.

Table 4. the experimental results of the stress intensity factor according to Eq. (1) for the specimen.

Thickness (mm)	Force (kN)	CMOD (mm)	K_I (MPa$\sqrt{m}$)	K_I average (MPa$\sqrt{m}$)
15	0.502	0.002	10.729	75.412
	0.953	0.018	32.188	
	4.586	0.084	69.534	
	9.175	0.209	109.682	
	12.606	0.417	154.927	

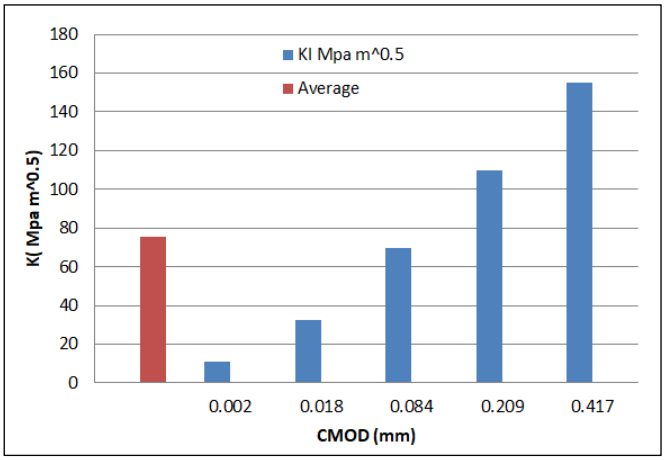

Fig. 22 the relationship between stress intensity factor K_I and CMOD.

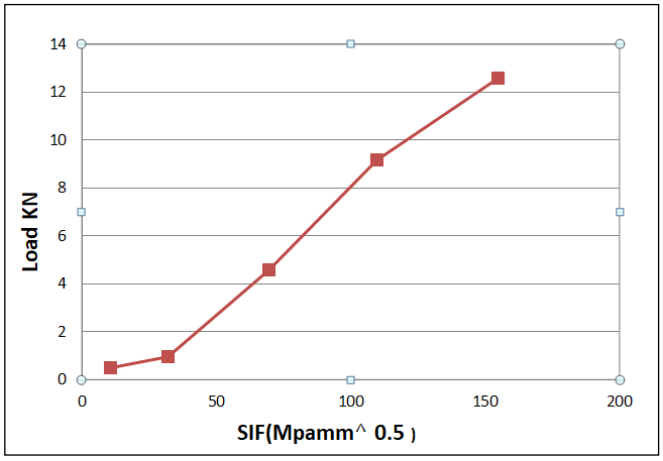

Fig. 23 the relationship between load and stress intensity factor SIF.

6. Numerical result

6.1. Ansys stresses result

The results obtained by Finite Element Analysis present maximum stress of 643.77 MPa located at the crack tip edge. Fig. 24 shows a compact specimen and the stress distribution at the specimen body. The stress distribution around the notch is approximate 416.69 MPa and in a small zone near the crack tip edge, the stress concentration reaches the maximum stress.

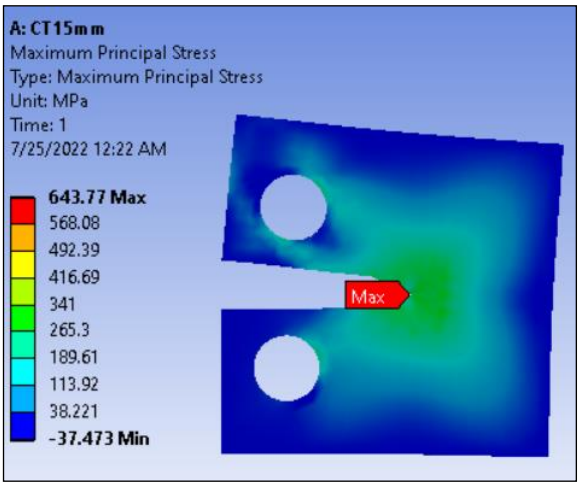

Fig. 24 Stress distribution in compact specimen.

Taking a close image of the crack tip where are concentrated the maximum stresses, is located a small zone around the crack tip edges where the stresses come to around 518.6 MPa. This zone is known as the plastic deformation zone as shown in Fig. 25.

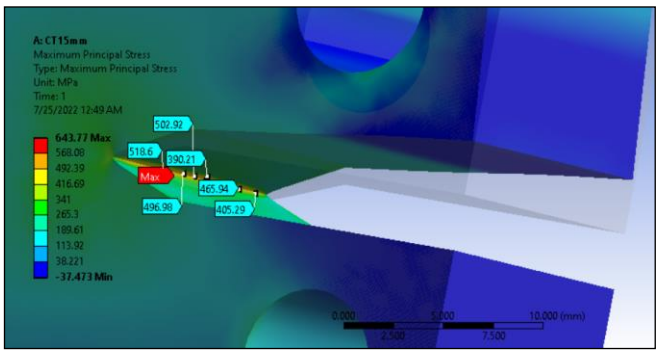

Fig. 25 lose image of crack tip notch surface.

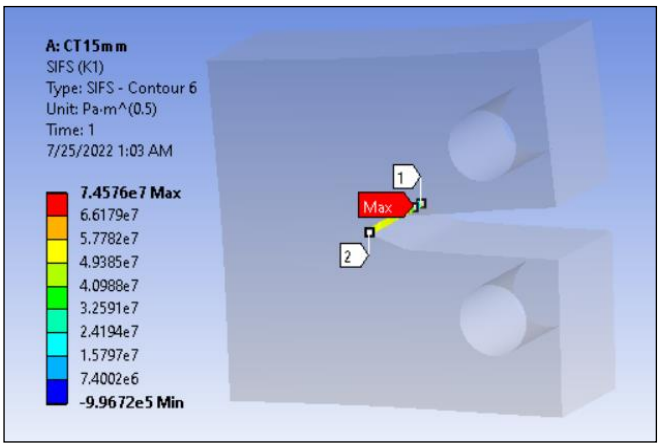

Fig. 26 Stress intensity factor magnitude in the compact specimen.

The stress intensity factor inside the compact specimen is shown in detail in Fig. 27. It shows the lower intensity parameters near the crack's outside edges.

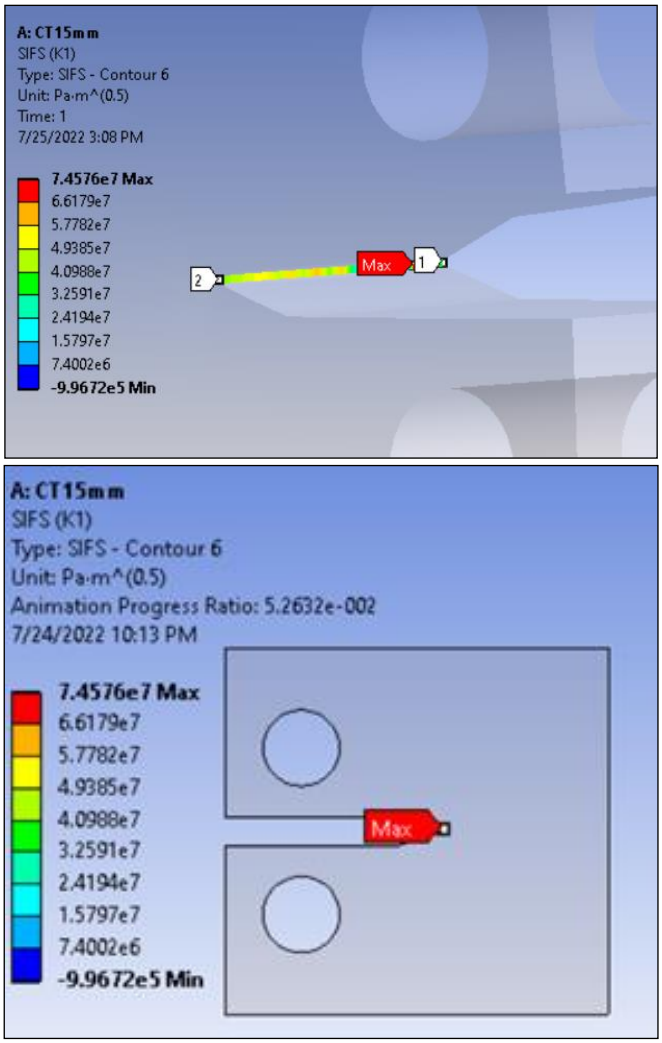

Fig. 27 Stress intensity factor K_I at the crack tip.

6.2. Comparison between experimental K and K_I

The non-linear three-dimensional finite element model according to ASTM E-399-12 specification gave excellent results for the prediction of stress intensity factor directly from ANSYS software as shown in Table 4.

Table 4. Differences between experiments and FEA result in the prediction of stress intensity factors.

Thickness (mm)	Experiment K_I (MPa$\sqrt{m}$)	K_I by FEA (MPa$\sqrt{m}$)	Error (%)
15	75.412	74.576	1.121

Where for 15 mm thickness, the stress intensity factor predicted from the experimental result for compact tension specimen was about 75.412 MPa$\sqrt{m}$, while the stress intensity factor K_I predicted by the finite element model at load 12.606 kN directly from ANSYS software was about 74.576 MPa$\sqrt{m}$. The errors between experimental and finite element results for stress intensity factor value were about 1.12 %. Distribution of von miss and deformation in compact tension specimen as shown in Fig. 28 and 29 respectively.

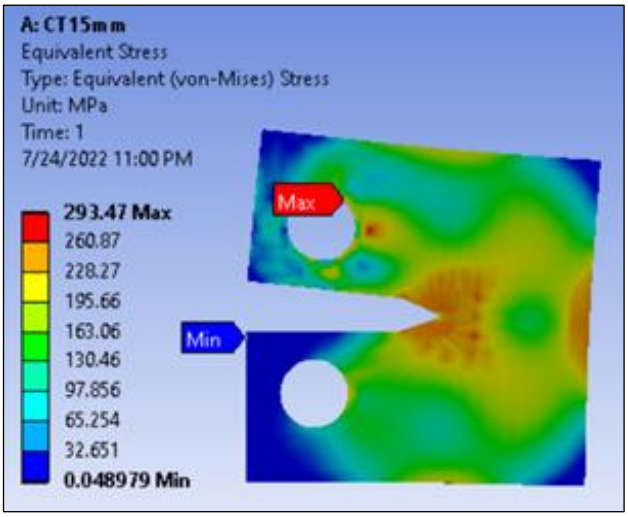

Fig. 28 Distribution of von miss in compact tension specimen.

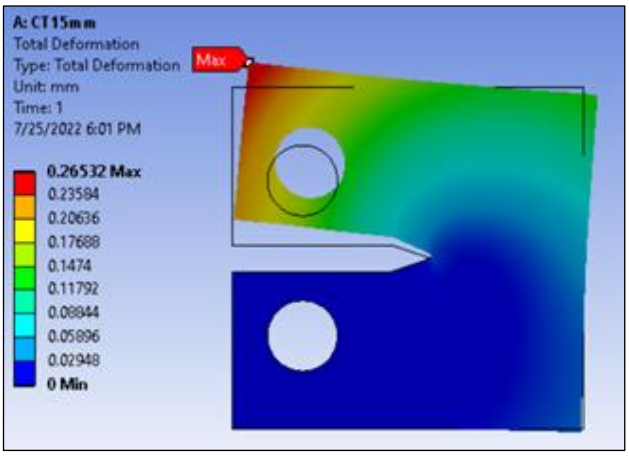

Fig. 29 Total deformation on the specimen.

7. Conclusions

In this work, the stress intensity factor K_I characterization was realized in structural steel low carbon steel according to ASTM E-399-12 of linear elastic region fracture mechanics. Prediction of stress intensity factor and crack mouth opening displacement for standard test *CT* specimens has been carried out experimental and numerical by finite element analysis using ANSYS workbench R19 software results are good arguments with experimental values which gives knowledge of how stress intensity factor varies with CMOD and load, also how CMOD varies with the load.

Based on the results obtained, the following conclusions can be made:

1. The average K_I value obtained during the experiment was 75.412 MPa$\sqrt{m}$.
2. The K_I value obtained during the FEA was 74.576 MPa$\sqrt{m}$.
3. The stress intensity factor K_I remains very close between experimental and FEA in the elastic region with an error percentage of about 1.12 %.
4. The experimental mechanical properties, yield stress is 287.8 MPa and ultimate tensile stress is 433.6 MPa, have a good agreement with the value in the stander of this material.
5. In mode I the stress intensity factor K_I increases with increasing load until reaches a critical load value during the linear region.
6. CMOD that is affected by the load when load increase leads to an increase in CMOD and when the load reaches the critical value, the load starts to decrease with constant CMOD or a slight increase, according to the increase in CMOD, the stress intensity factor increases.

References

[1] ASTM E399, "Standard Test Method for Linear-Elastic Plane-Strain Fracture Toughness K_{IC} of Metallic Materials", 2013.

[2] F. Bozkurt and E. Schmidová, "Fracture Toughness Evaluation of S355 Steel Using Circumferentially Notched Round Bars", Vol. 47, Issue 2, pp. 91-95, 2019. https://doi.org/10.3311/PPtr.11560

[3] S. İriç, O. Demir and A. O. Ayhan, "Applicability of compact tension specimens for evaluation of the plane-strain fracture toughness of steel", Materials Testing, Vol. 61, No. 12, pp. 1220-1224, 2019. https://doi.org/10.3139/120.111436

[4] A. A. Nassar and E. G. Fayyad, "Linear and Non-Linear Stress Analysis for the Prediction of Fracture Toughness for Brittle and Ductile Material using ASTM E399 and ASTM E1290 by ANSYS Program Package", IOP Conference Series: Materials Science and Engineering, Vol. 579, 2019. https://doi.org/10.1088/1757-899X/579/1/012050

[5] D. M. Kulkarni, R. Prakash, and A. N. Kumar, "Experimental and finite element analysis of fracture criterion in general yielding fracture mechanics", Sadhana, Vol. 27, pp. 631-642, 2002. https://doi.org/10.1007/BF02703355

[6] D. Ping, Z. Pengcheng and L. Ruiwen, "Study on Stress Distribution Near Crack Tip in Beryllium Compact Tension Specimen", 12th A-PCNDT 2006 – Asia-Pacific Conference on NDT, 5th – 10th Nov. 2006, Aukland, New Zealand.

[7] M. K. S. K. Nagoju, "Computation of Stress Intensity Factor and Critical Crack Length of ASTM A36 Steel using Fracture Mechanics", International Journal of Engineering Research & Technology (IJERT), Vol. 2, Issue 9, 2013.

[8] Z. M. Beltrán, S. F. Hernández, L. D. Rivas, V. J. L. González, R. H. Dorantes, "Fracture Toughness Characterization", International Journal of Engineering Research and Applications, Vol. 4, Issue 11, pp. 60-66, 2014.

[9] R. Sołtysiak, D. Boroński, and M. Kotyk, "Experimental verification of the crack opening displacement using finite element method for CT specimens made of Ti6Al4V titanium alloy", AIP Conference Proceedings, Vol. 1780, 2016. https://doi.org/10.1063/1.4965953
[10] M. J. Abdulsada, "Experimental and Numerical Study of Mechanical Properties and Fracture Mechanics Analysis of AISI1010 Low Carbon Steel Welded Joints", M.Sc. Thesis, Mechanical Engineering Department, College of Engineering, University of Basrah, Basrah, Iraq, 2018.
[11] F. Wester and E. Gunnarsson, "3-D Modelling of Plane-Strain Fracture Toughness Tests using Ansys Workbench", M.Sc. Thesis, Department of Mechanics and Maritime Sciences, Chalmers University of Technology, Gothenburg, Sweden, 2020.
[12] Y. K. Khdir, "The Determination of the Stress Intensity Factors of a Steel Plate with Different Thickness using Fem", the Journal of Duhok University, (Special Issue) Third International Conference on Recent Innovations in Engineering (ICRIE) Duhok, Vol. 23, No. 2, pp. 679-692, 2020. https://doi.org/10.26682/csjuod.2020.23.2.53
[13] O. B. Chan, A. E. Elwi and G. Y. Grondin, "Simulation of Crack Propagation in Steel Plate with Strain Softening Model", Structural Engineering Report No. 266, University of Alberta, Department of Civil and Environmental Engineering, Edmonton, Alberta, 2006.
[14] M. S. Kahyoosh, R. M. Laftah, and A. A. Nassar, "Effect of Fiber Orientation Angle on Stress Intensity Factor of Composite Plate using Extended Finite Element Method (XFEM)", Basrah Journal for Engineering Sciences, Vol. 22, Issue 1, pp. 58-68, 2022. https://doi.org/10.33971/bjes.22.1.7
[15] N. A. H. Saleh, "A Study on Second Mode Stress Intensity Factor (K_{II}) of Cracked Plates under Compression Load", Basrah Journal for Engineering Science, Vol. 12, Issue 2, pp. 54-65, 2012.
[16] A. H. Taha and A. A. Nassar, "Determination of the (Δ-R) and (J-R) Curves for Pressure Vessel Material EN AW-5083 using Stepped Notched Compact Tension Specimen (CT)", 2015. https://doi.org/10.17605/OSF.IO/3S95N
[17] ASTM E8/E8M-22 Standard, "Standard Test Methods for Tension Testing of Metallic Materials", 2013.
[18] T. L. Anderson, Fracture Mechanics Fundamental and Applications, Second Edition, CRC Press 2005.
[19] C. Bayley, "Evaluation of the single edge notch tension specimen for quantifying fracture toughness participation in a round-robin test program", 2015.